PRAMANA — journal of physics

Vol. 79, No. 4
October 2012
pp. 541–553

Standard Model Higgs boson searches with the ATLAS detector at the Large Hadron Collider

ALEANDRO NISATI, on behalf of the ATLAS Collaboration
INFN, Via Anagnina 317, 00118 Rome, Italy
E-mail: nisati@cern.ch

Abstract. The investigation of the mechanism responsible for electroweak symmetry breaking is one of the most important tasks of the scientific program of the Large Hadron Collider. The experimental results on the search of the Standard Model Higgs boson with 1 to 2 fb^{-1} of proton–proton collision data at $\sqrt{s} = 7$ TeV recorded by the ATLAS detector are presented and discussed. No significant excess of events is found with respect to the expectations from Standard Model processes, and the production of a Higgs boson is excluded at 95% Confidence Level for the mass regions 144–232, 256–282 and 296–466 GeV.

Keywords. Higgs; Standard Model; ATLAS.

PACS Nos 14.80.Bn; 12.15.Ji; 13.85.Rm

1. Introduction

The search for the Standard Model (SM) Higgs boson is one of the most important priorities of the Large Hadron Collider (LHC) scientific programme. A recent review of the theory of the SM Higgs is available in [1]. Direct searches at the CERN LEP collider exclude the existence of this boson with its mass m_{H} lower than 114.4 GeV [2]. Searches by the CDF and D0 experiments at the Fermilab $p\bar{p}$ collider have explored the Higgs boson mass up to 200 GeV. The most recent results on this search at the Tevatron collider were presented in this conference [3].

Early results on SM Higgs boson searches recently performed by the ATLAS and CMS experiments at the LHC, using data samples of proton–proton collisions at $\sqrt{s} = 7$ TeV corresponding to an integrated luminosity from 1 to 2 fb^{-1}, are also available.

In this paper, the results on this search from the ATLAS detector [4] are presented. The results on the study performed by CMS are available in [5]. The channels analysed by ATLAS to search for this boson are summarized in table 1.

The following sections describe in some detail the results achieved in each of these channels. Particular attention is given to the decay channels $H \to \gamma\gamma$, $H \to WW^{(*)} \to l\nu l\nu$ and $H \to ZZ^{(*)} \to 4l, ll\nu\nu$ as they play important roles in setting the overall result of this study. The analyses take into account the main systematic experimental effects,

DOI: 10.1007/s12043-012-0360-z; ***e*Publication: 22 September 2012**

Table 1. The Higgs boson decay channels studied by ATLAS and reported in this paper (the results on the study of the decay channel $H \to WW^{(*)} \to l\nu qq$, available in [14], are neither included in this paper, nor in the overall statistical combination described in the last section). The integrated luminosity related to each of the processes analysed is also given.

Decay channel	Integrated luminosity (fb^{-1})	Mass range search (GeV)
$H \to \gamma\gamma$ [6]	1.08	110–150
$W, ZH \to l\nu, ll\, b\bar{b}$ [7]	1.04	110–130
$H \to \tau^+\tau^-$ [8,9]	1.06	110–150
$H \to WW^{(*)} \to l\nu l\nu$ [10]	1.70	110–300
$H \to ZZ^{(*)} \to llll$ [11]	2.1	110–600
$H \to ZZ \to ll\nu\nu$ [12]	1.04	200–600
$H \to ZZ \to llqq$ [13]	1.04	200–600

such as those related to the calibration and reconstruction efficiencies of electrons, muons, tau decays to hadronic final states, jets, transverse missing energy and b-tagging. Theory uncertainties associated with background processes as well as with the Higgs boson signal are also taken into account. The relative uncertainty in the measurement of integrated luminosity, $\Delta L/L = 3.7\%$, is also included. The theory uncertainties in the production cross-section and decay branching fractions of the Higgs boson are taken from [15].

No significant excess of events is found with respect to the expectations from Standard Model processes, and hence exclusion limits on the production cross-section are set at 95% confidence level (CL) with a statistical analysis based on the CLs [16] method, using the profile likelihood ratio [17] as test statistic. Finally, the statistical combination of the findings from each channel is presented and discussed in the last section.

2. $H \to \gamma\gamma$

The $H \to \gamma\gamma$ decay represents one of the few Higgs processes, whose final state can be fully reconstructed experimentally. Despite the low branching ratio, $\text{BR}(H \to \gamma\gamma) \approx 2 \times 10^{-3}$ for a Higgs boson with mass $m_{\text{H}} = 120$, this channel provides good experimental sensitivity in the mass region below 150 GeV [6]. The production cross-section of this process is about 0.04 pb.

The background to this final state can be subdivided into two classes: irreducible and reducible. The irreducible background is made by direct production of diphoton events from the scattering of the initial proton constituents, that can be described by Born, bremsstrahlung and box Feymann diagrams. The inclusive cross-section is about 30 pb. The theoretical prediction is calculated at the next-to-leading order (NLO) and it is known with an uncertainty of about 20%. The reducible background is made by γ-jet and jet–jet QCD processes, where one or two jes are misidentified as photons, respectively.

The excellent performance of the ATLAS electromagnetic calorimeter is able to ensure a good jet-photon separation, thanks in particular to the fine granularity along the

pseudorapidity η. This allows to strongly reduce the level of contaminations due to the misidentified photon background arising from jet production. In the offline reconstruction, photons are classified as 'unconverted' (electromagntic calorimeter clusters with no matching with tracks in the Inner Detector) and 'converted' (clusters that match with a track pair, or a single track, consistent with a photon conversion in the material of the Inner Detector). The single photon reconstruction efficiency is ≈98%, while the identification efficiency ranges typically from 75 to 90% for photon transverse energies between 25 and 100 GeV. The purity of the sample (fraction of genuine diphoton events) is about 72%. After selection, the fraction of candidates with at least one converted photon is 64%.

Events with two isolated high-quality photons are selected in the pseudorapidity range $\eta < 1.37$ and $1.52 < |\eta| < 2.37$, with $p_{\mathrm{T}} > 40$ GeV for the leading photon and $p_{\mathrm{T}} > 25$ GeV for the subleading photon. An accurate mass reconstruction is mandatory to maximize the signal-to-background ratio, and hence have a good sensitivity to $\gamma\gamma$ resonances. The reconstructed width of the Higgs boson peak is expected to be fully dominated by the experimental resolution. The experimental resolution is composed of single-photon energy measurement accuracy, as well as of the diphoton opening angle in space. For most of the $H \to \gamma\gamma$ topologies, the angular resolution plays an important role, and therefore it is important to get an accurate measurement of the photon direction of flight. The ATLAS electromagnetic calorimeter also measures the photon flight direction with an angular resolution, in case of unconverted photons, of about 14 mrad at $\eta = 0$, a factor ≈4 smaller than the accuracy that is obtained using the average pp interaction point and its spread. An even better resolution is achieved if at least one of the two photons is converted. This allows to obtain a $\gamma\gamma$ invariant mass resolution $\delta(m_{\gamma\gamma}) \sim 1.7$ GeV at $m_{\gamma\gamma} = 120$ GeV, dominated by the photon energy resolution. The analysis is then performed by classifying the selected events in five complementary categories, depending on whether none, one or both photons are converted, and on their measured pseudorapidity. For each category, the $m_{\gamma\gamma}$ invariant mass distribution is fitted with an exponential falling distribution to describe the background continuum, superimposed on a 'crystal-ball' function representing the Higgs boson signal.

The number of selected events in the 100–160 GeV mass range is found to be 4846, whose measured number of diphoton events is $3650 \pm 100 \pm 290$. The first uncertainty is statistical, and the second is systematic, arising from the estimation made with the control region. Figure 1a shows the reconstructed invariant mass spectrum.

The total relative systematic uncertainty on the expected signal yield is 12%, dominated by the photon reconstruction and identification efficiency. The uncertainty on the background measurement is between five events at $m_{\mathrm{H}} = 110$ GeV and three events at $m_{\mathrm{H}} = 150$ GeV, in a mass interval of 4 GeV. No evidence of a significant excess of events on top of the background level is found. Exclusion limits on the inclusive production cross-section of a Standard Model-like Higgs boson relative to the Standard Model cross-section are derived. The result, including systematic uncertainties, are shown in figure 1b. The observed limit on the cross-section production ranges between 2.0 and 5.8 times those predicted by the SM. The expected median limit when there is no signal, varies from 3.3 to 5.8 times the SM predictions. The expected and the observed limits vary within less than two sigma in the full mass interval analysed.

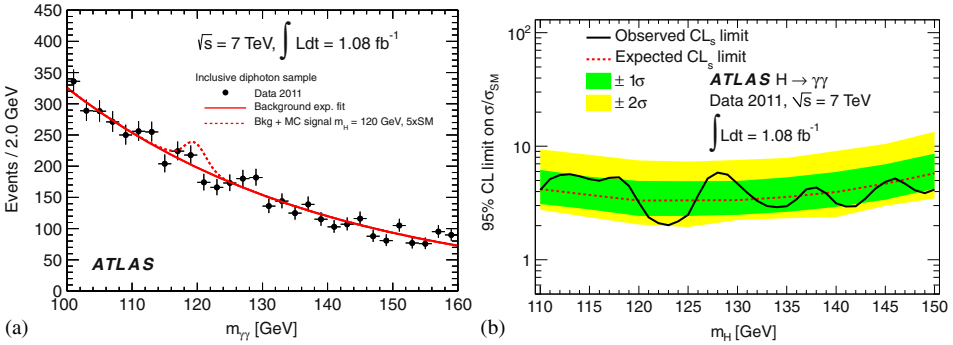

Figure 1. (**a**) Distribution of the reconstructed invariant mass. The exponential fit to the full data sample of the background only hypothesis, as well as the expected signal for a Higgs boson of 120 GeV, mass with five times the production cross-section, are also shown. (**b**) 95% confidence level upper limit on a Standard Model-like Higgs boson production cross-section, normalized to the SM prediction, as a function of the Higgs boson mass. The solid line describes the observed limit, while the dashed line shows the median expected limit assuming no Higgs boson. The bands indicate the expected fluctuation around this limit at 1 and 2σ levels [6].

3. $W/Z + H$, $H \to b\bar{b}$ and $H \to \tau^+\tau^-$

The $H \to b\bar{b}$ decay is of particular importance as it is one of the few channels that offers the possibility of measuring directly the Higgs couplings to quarks. It also plays an important role in the search of this boson in the mass region below 140 GeV. It is the dominant Higgs decay at low mass, but the QCD jet background makes this search in the inclusive channel impossible. On the contrary, it is promising in the associated production with gauge bosons W, Z. ATLAS has performed an analysis, based on an integrated luminosity of $L = 1.04$ fb^{-1}, searching for $H \to b\bar{b}$ produced in association with a W or a Z. The leptonic decay of the boson is used both for trigger and offline event preselection. The analysis proceeds requiring exactly two b-tagged jets [18] with $p_{\mathrm{T}} > 25$ GeV. The $t\bar{t}$ production and single top are the dominant backgrounds in the WH channel; other important backgrounds are $W+$jets and QCD multijet production. The $Z+$jets production is the dominant background in the ZH channel; other important backgrounds are $t\bar{t}$ and diboson production. The study focusses on the analysis of the jet–jet invariant mass $m_{b\bar{b}}$, where the Higgs signal should appear as a bump on top of the background continuum. Figure 2a shows the distribution of $m_{b\bar{b}}$ after all selection cuts, for the ZH associated production.

In this study, the background contributions are either measured directly from data, or evaluated from Monte Carlo (MC) simulations, and validated with data control samples. The total relative uncertainty on the overall background is about 9% for both associated production modes. The systematic uncertainty on the Higgs boson yield is dominated by the uncertainty on the b-tagging efficiency (about 17%); the uncertainty on the jet energy scale (JES) produces a relative uncertainty of about 8% on the signal yield.

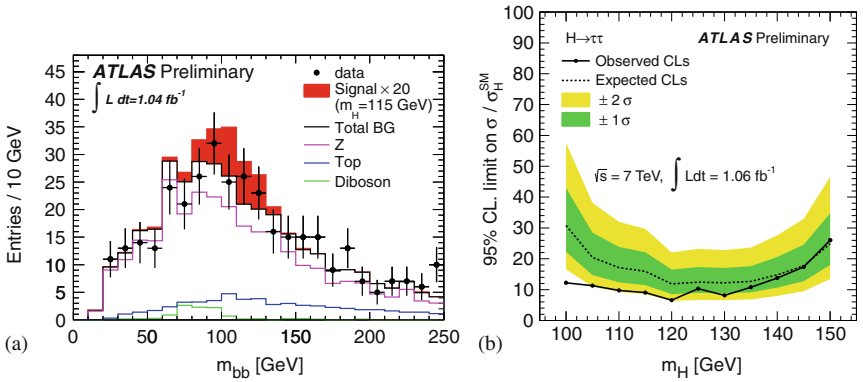

Figure 2. (**a**) The invariant mass, $m_{b\bar{b}}$, for $ZH \rightarrow llb\bar{b}$, after full analysis, for $m_{\mathrm{H}} = 115$ GeV. The signal is enhanced by a factor 20 [7]. (**b**) Expected and observed limits at the 95% CL, on the production of a Standard Model Higgs boson in the $\tau^+\tau^-$ final state, as a function of the mass m_{H} [8,9,21].

No event excess is found, and 95% CL exclusion limits are set as a function of the Higgs boson mass. In the mass range 110–130 GeV, a production cross-section of about 10–15 times the one predicted by the SM is excluded. The obseved limits are within about 1σ of the expected limits. More details of this analysis are available in [7].

The inclusive $H \rightarrow \tau^+\tau^-$ decay can be used for searches in the mass range $110 < m_{\mathrm{H}} < 140$ GeV. The vector boson fusion (VBF) process [1] offers the advantage of a small background, at the price of a low signal production rate. Three classes of final states are available, depending on the τ-lepton decay: lepton–lepton (ll), lepton–hadron (lh) and hadron–hadron (hh). ATLAS has studied the final states ll, produced in association with at least one high-p_{T} jet and lh [8,9]. The most important backgrounds are represented by the production of W, $Z \rightarrow$ leptons + jets, $Z \rightarrow \tau^+\tau^-$ (largely irreducible), dibosons, $t\bar{t}$, single top and jets. The analysis is based on the selection of high-p_{T} leptons and of at least one jet. The collinear approximation [19] (missing mass calculator [20]) is adopted to reconstruct the tau momentum in the $ll(lh)$ decay mode. The $\tau\tau$ system invariant mass is studied to search for the Higgs signal.

The background contamination in the selected event sample is evaluated using methods based on measurements from data, or on predictions from Monte Carlo simulation. The overall uncertainty on the background level in the ll final state is 8%, while for lh it is 19%.

No event excess is found, and an exclusion limit on the Higgs production cross-section is set (see figure 2b).

4. $H \rightarrow WW^{(*)} \rightarrow lvlv$

The $H \rightarrow WW^{(*)} \rightarrow lvlv$ decay is the most sensitive Higgs decay in the mass range $130 < m_{\mathrm{H}} < 200$ GeV. At the same time, this is also one of the most challening channels, as the complete reconstruction of the invariant mass of this final state is not

possible because of the presence of neutrinos. The dominant background originates from the irreducible SM W^+W^- production. Other important background processes are QCD multijet, W + jets, Drell–Yan and top quark production. The analysis is based on the preselection of two isolated high-p_{T} opposite sign leptons and large missing transverse energy $E_{\mathrm{T}}^{\mathrm{miss}}$. The leading lepton is required to have $p_{\mathrm{T}} > 25$ GeV, the subleading lepton $p_{\mathrm{T}} > 20$ GeV if it is an electron, 15 GeV if it is a muon. QCD and Drell–Yan backgrounds are suppressed by a $E_{\mathrm{T}}^{\mathrm{miss}}$ requirement studying the quantity $E_{\mathrm{T,rel}}^{\mathrm{miss}}$, defined as the reconstructed $E_{\mathrm{T}}^{\mathrm{miss}}$ if the absolute azimuthal angle $\Delta\phi$ between the $E_{\mathrm{T}}^{\mathrm{miss}}$ vector and the nearest lepton (jet) with $p_{\mathrm{T}} > 15(25)$ GeV is $\Delta\phi \geq \pi/2$, otherwise $E_{\mathrm{T,rel}}^{\mathrm{miss}} = E_{\mathrm{T}}^{\mathrm{miss}} \cdot \sin\Delta\phi$. The analysis proceeds after classifying the events into two categories: the 0-jet and the 1-jet bins, depending on whether exactly one jet with $p_{\mathrm{T}} > 25$ GeV in the region $|\eta| < 4.5$ has been reconstructed or not. Events with two or more jets are not considered in this analysis. For 1-jet bin selection, b-tagged jets are vetoed. The b-tagging algorithm uses a combination of impact parameter significance and the topology of weak b- and c-hadron decays (the b-tagging probability of the algorithm used in this analysis to identify b-jets in $t\bar{t}$ events is 70%). Additional cuts on the transverse momentum of the dilepton system, on the jet energy and on the missing transverse energy are made, as well as cuts to reject $Z \to \tau\tau$ decays. Topological cuts based on the measurements of the lepton–lepton invariant mass, transverse momentum and opening angle in the transverse plane, are also made for both event selections (for more details, see [10]).

The 'transverse mass' m_{T}, defined as $m_{\mathrm{T}} = [(E_{\mathrm{T}}^{ll} + E_{\mathrm{T}}^{\mathrm{miss}})^2 - (\mathbf{P}_{\mathrm{T}}^{ll} + \mathbf{P}_{\mathrm{T}}^{\mathrm{miss}})^2]^{1/2}$, where $\mathbf{P}_{\mathrm{T}}^{ll}$ is the transverse momentum of the dilepton system and E_{T}^{ll} is its associated energy,

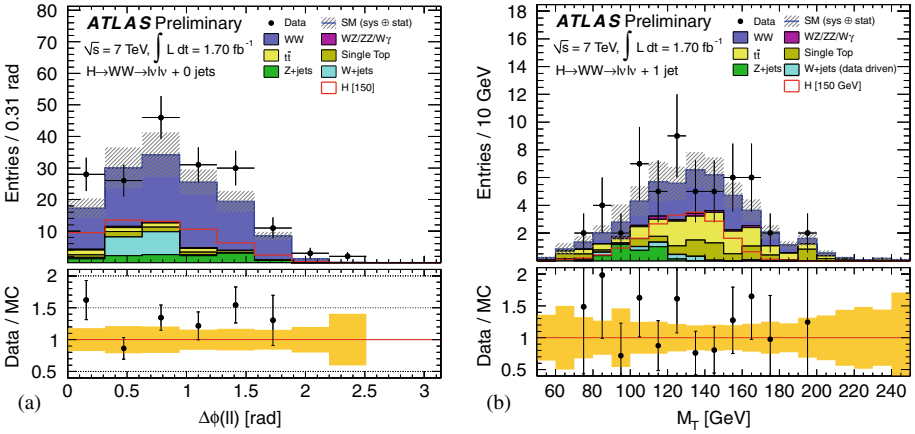

Figure 3. (**a**) $H \to WW^{(*)} \to l\nu l\nu$ selection, 0-jet bin: the azimuthal opening angle $\Delta\phi_{ll}$ of the two selected leptons after preselection cuts, the lepton–lepton transverse momentum and invariant mass cuts. (**b**) $H \to WW^{(*)} \to l\nu l\nu$ selection, 1-jet bin: the transverse mass m_{T} distribution after all cuts except for the cut on m_{T} itself. For both plots the expected signal is shown for $m_{\mathrm{H}} = 150$ GeV. Also, the lower part of these plots shows the ratio between the data and the MC prediction. The yellow band indicates the total systematic uncertainty [10].

Table 2. The number of background events, in the 0-jet and 1-jet bins, expected from Standard Model processes, observed in the data, and expected from the production of a Higgs boson with $m_{\mathrm{H}} = 150$ GeV, using an integrated luminosity of 1.7 fb^{-1}. The uncertainties shown are the combination of the statistical and all systematic uncertainties, including the ones from the background extrapolations from control to signal regions [10].

Category	WW	$t\bar{t}$	Total SM background	Data	Higgs
0-jet	43 ± 6	2.2 ± 1.4	53 ± 9	70	34 ± 7
1-jet	10 ± 2	6.9 ± 1.9	23 ± 4	23	12 ± 3

is reconstructed and used for the final selection: for a given Higgs mass hypothesis m_{H}, events satisfying the condition $0.75 \cdot m_{\mathrm{H}} < m_{\mathrm{T}} < m_{\mathrm{H}}$ are accepted. Figure 3a shows for the 0-jet selection, the distribution of the lepton–lepton azimuthal opening angle. Figure 3b shows the m_{T} distribution for the 1-jet selection.

It is important to estimate the background contamination in the signal region by measuring the data control samples. In the analysis presented in this document, the three largest background contributions to this channel, from $WW^{(*)}$, top and W+jets, are evaluated using the collision data. For the remaining smaller background contributions, Monte Carlo predictions are used. The number of events counted in control regions enriched by a given SM process are propagated to the signal region through an extrapolation factor evaluated with MC samples. Extrapolation factors are evaluated for $WW^{(*)}$ and top processes, while the $W+$ jet contamination is fully measured in data. Table 2 reports the number of events expected from Standard Model processes, as well as from a Higgs boson with mass of $m_{\mathrm{H}} = 150$ GeV. These numbers are compared to the observed numbers of

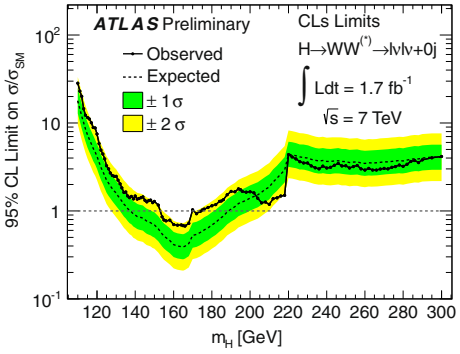

Figure 4. The expected (dashed line) and observed (solid line) 95% CL upper limits on the production cross-section from $H \to WW^{(*)} \to l\nu l\nu$ normalized to the Standard Model prediction, as a function of the Higgs boson mass. The observed limits at neighbouring mass points are highly correlated due to the limited mass resolution of this final state. The bands indicate the 1σ and 2σ uncertainty regions on the expected limit. The jump visible at $m_{\mathrm{H}} = 220$ GeV is due to the change of the selection criteria at that mass point [10].

events in each category. The main uncertainties on the $WW^{(*)}$ and top quark production background contribution to the selected events are due to the accuracy of the extrapolation of their measurement from the control regions to the signal region. They account for the effects to the limited knowledge of the JES, b-tagging efficiency, as well as the renormalization and factorization scales, and the parton distribution functions associated with the theory models used to perform these extrapolations. The uncertainty on the Higgs boson signal yield is 5% in the 0-jet bin and 12% in the 1-jet bin.

No significant excess of events is found, and therefore an exclusion limit on the production cross-section of a Standard Model-like Higgs boson is set.

Figure 4 shows the observed and expected limits at 95% CL for the combined 0-jet and 1-jet analyses as a function of the Higgs boson mass. A SM Higgs boson is excluded in the mass interval $154 < m_{\mathrm{H}} < 186$ GeV, while the expected Higgs boson exclusion mass interval is $135 < m_{\mathrm{H}} < 196$ GeV. The largest observed difference between the observed and the expected limit is less than 2σ.

5. $H \to ZZ \to llvv$ and $H \to ZZ \to llqq$

The $H \to ZZ \to llvv$ decay is characterized by a final state where two leptons are produced in association with large transverse missing energy. This decay mode offers a significant branching fraction in combination with a good separation from background processes. These processes are mainly the irreducible diboson production WW, WZ and ZZ, plus the reducible background processes represented by top quark final states, as well as $W, Z+$jets. The analysis proceeds with the selection of two isolated same-flavour opposite charge high-p_{T} leptons whose invariant mass is consistent with the Z-mass, and large $E_{\mathrm{T}}^{\mathrm{miss}}$. Toplogical cuts are applied to suppress the $W, Z+$jets background. Finally the transverse mass distribution m_{T}, defined as

$$m_{\mathrm{T}}^2 = \left(\sqrt{m_{\mathrm{Z}}^2 + |\mathbf{p}_{\mathrm{T}}^{ll}|^2} + \sqrt{m_{\mathrm{Z}}^2 + |\mathbf{p}_{\mathrm{T}}^{\mathrm{miss}}|^2}\right)^2 + (\mathbf{p}_{\mathrm{T}}^{ll} + \mathbf{p}_{\mathrm{T}}^{\mathrm{miss}})^2 \tag{1}$$

is studied to search for contributions from the production and decay of the SM Higgs boson ($\mathbf{p}_{\mathrm{T}}^{\mathrm{miss}}$ is the missing transverse energy vector).

The systematic uncertainties include experimental uncertainties related to the calibration and reconstruction efficiencies of electrons, muons, jets and b-jets that are propagated also the reconstruction of $E_{\mathrm{T}}^{\mathrm{miss}}$. Uncertainties relative to the Higgs signal yield prediction (about 12% for the gluon–gluon production and 4% for the VBF) as well as to the ZZ background (11%), have also been taken into account.

The observed m_{T} distribution is consistent with the expectations from Standard Model processes. Exclusion limits at 95% CL have been set as a function of the Higgs boson mass. The results are shown in figure 5a. The Standard Model Higgs boson with mass in the region $340 < m_{\mathrm{H}} < 450$ GeV is excluded. The expected limit is lowest around $m_{\mathrm{H}} = 380$ GeV where it is 1.1 times the cross-section predicted by the SM. The observed and expected limits agree within 2σ over the entire mass range. The details of this analysis are in [12].

Another channel important for high-mass SM Higgs boson searches is the $H \to ZZ \to llqq$ decay, also characterized by a large branching fraction. The event selection is based

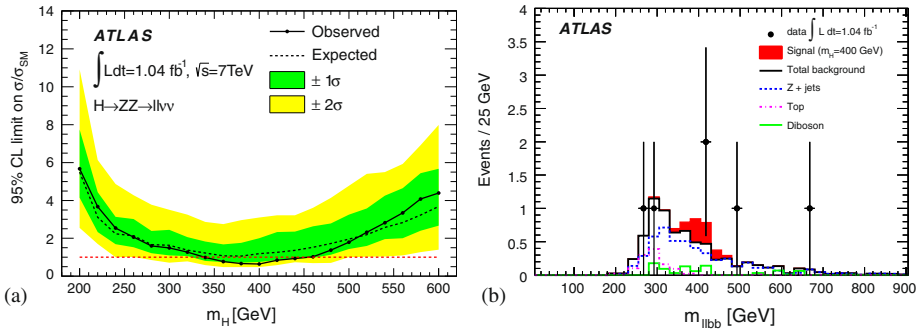

Figure 5. (**a**) Observed (solid line) and expected (dashed line) 95% CL upper limits on the Higgs boson production cross-section divided by the SM prediction for the $H \to llvv$ search. The green and yellow bands indicate the 1σ and 2σ fluctuations, respectively, around the median sensitivity [12]. (**b**) The invariant mass of the $lljj$ system for the channel obtained by the $H \to ZZ \to llqq$ search analysis. The expected Higgs boson signal for $m_{\mathrm{H}} = 400$ GeV is also shown [13].

on the reconstruction of final states with two same-flavour opposite-charge high-p_{T} leptons, whose invariant mass is consistent with the Z boson mass m_{Z}, in association with two high-p_{T} jets again with an invariant mass consistent with m_{Z}, and no significant transverse missing energy. The distribution studied for the Higgs boson search is obviously the two-lepton and two-jet system invariant mass. This distribution is studied also for events with both b-tagged jets [18]. The dominant background is the irreducible ZZ production, the reducible WZ, Z, $W+$jets and QCD jets. The Higgs boson signal would appear as a bump on top of the expected background (see figure 5b). No significant excess is observed, and therefore exclusion limits of 95% CL production cross-section are set. The production cross-section about 1.7 times the one predicted by the SM is excluded for $m_{\mathrm{H}} \sim 360$ GeV. The expected limit is between 2.7 and 9 the SM cross-section in the mass range 200 to 600 GeV. The details of this analysis are in [13].

6. $H \to ZZ^{(*)} \to llll$

Three distinct channels are studied in this analysis: $H \to ZZ^{(*)} \to e^+e^-e^+e^-$, $\mu^+\mu^-\mu^+\mu^-$, $e^+e^-\mu^+\mu^-$. The production of SM $ZZ^{(*)}$ dibosons represents the irreducible background. Processes such as $Z+$jets (in particular $Zb\bar{b}$) and $t\bar{t}$, where at least two fake/non-prompt leptons are reconstructed from jets or heavy quark semi-leptonic decays, represent the more important reducible backgrounds to these final states. Data have been selected using single-lepton triggers. In the offline analysis, events with two pairs of same-flavour opposite-sign isolated leptons are selected. Each lepton must have $p_{\mathrm{T}} > 7$ GeV; electrons (muons) should lie in the region $|\eta| < 2.47(2.50)$. The electron p_{T} threshold is increased to 15 GeV if the associated pseudorapidity is between $1.37 < |\eta| < 1.52$. At least two leptons must have $p_{\mathrm{T}} > 20$ GeV. The two lowest p_{T} leptons in events with the 4-lepton invariant mass of $m_{4l} < 190$ GeV are required to be tightly

associated with the primary vertex with cuts to the impact parameter significance (defined as the transverse impact parameter to the primary vertex divided by its uncertainty).

The invariant mass m_{12} of the lepton pair closest to the Z mass must fulfill $|m_{12}-m_{\mathrm{Z}}| < 15$ GeV. The invariant mass m_{34} of the other pair is required to be lower than 115 GeV and greater than a threshold depending on the reconstructed 4-lepton mass. The full-width half-maximum (FWHM) of the reconstructed Higgs particle, expected to be dominated by the experimental mass resolution for low m_{H} values, varies between 4.5 (4μ) GeV and 6.5 GeV ($4e$) for $m_{\mathrm{H}} = 130$ GeV. At high m_{H}, the reconstructed width is dominated by the intrinsic width (e.g. FWHM = 35 GeV for $m_{\mathrm{H}} = 400$ GeV). The expected contribution from SM background is estimated using Monte Carlo simulation, except the $Z+$jets process whose contribution is measured in data. The irreducible $ZZ^{(*)}$ process is predicted with an uncertainty of 15% (includes both quark–quark, quark–gluon and gluon–gluon scattering), while the top estimation, predicted with an uncertainty of 10%, is validated with data control samples. The $Z+$jet(s) contribution is evaluated starting from a sample of $Z+$lepton-pair selected with no isolation or impact parameter requirements. This yield is then extrapolated to the signal region applying reduction factors estimated with MC simulation. The uncertainty on the event contamination from this source varies in the range 20%–40%.

Figure 6a shows the distribution of the invariant mass of the selected candidates, compared to the expected contribution from SM processes. No significant excess of events has been found with respect to the SM prediction. Figure 6b shows the 95% CL exclusion limit on the production cross-section for the SM Higgs boson as a function of its mass. Details of the number of candidates selected in data and MC are illustrated in table 3. A SM Higgs boson with mass $191 < m_{\mathrm{H}} < 197$, $199 < m_{\mathrm{H}} < 200$ and $214 < m_{\mathrm{H}} <$

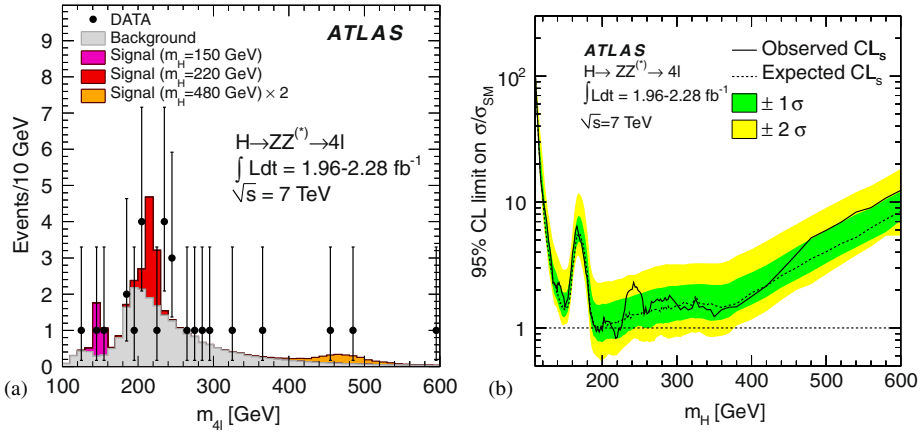

Figure 6. (**a**) Invariant mass distribution for the selected 4-lepton event candidates. The data are compared to the background expectations. (**b**) The expected (dashed line) and observed (solid line) 95% CL upper limits on the SM Higgs boson production cross-section, normalized to the SM prediction, as a function of its mass. Green and yellow bands indicate the fluctuations at 1σ and 2σ around the value of the median [11].

Table 3. The observed and expected number of events after full selection by the analysis for the $H \to ZZ^{(*)} \to 4l$ search [11].

Sample	4μ ($L = 2.28$ fb^{-1})	$2e2\mu$ ($L = 1.96$ fb^{-1})	$4e$ ($L = 1.98$ fb^{-1})
Observed	12	9	6
Expected	8.8 ± 1.2	11.1 ± 1.4	4.32 ± 0.52

224 GeV is excluded. The observed limits are consistent within the fluctuation less than 2σ with the expected ones. More details on this study are available in the paper recently submitted [11].

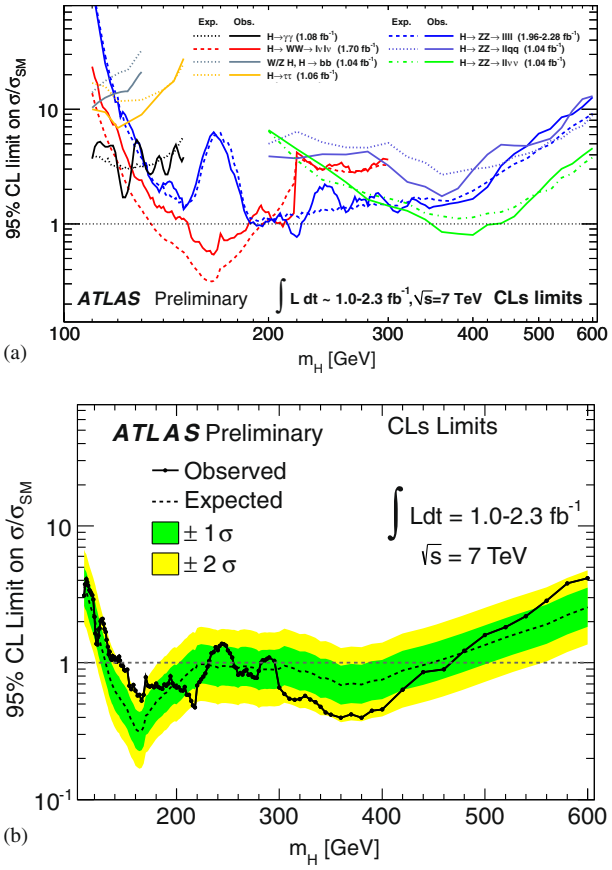

Figure 7. (**a**) The expected (dashed line) and observed (solid line) cross-section 95% exclusions limits for the individual search channels, normalized to the Standard Model Higgs boson cross-section, as functions of the Higgs boson mass. (**b**) The combined upper limit on the Standard Model Higgs boson production cross-section divided by the Standard Model expectation as a function of m_{H} is indicated by the solid line [21].

7. Overall SM Higgs combination

All channels presented in this paper are combined with a statistical procedure publicly available [22], which is again based on the modified frequentist method CLs [16]. The profile likelihood ratio is used as a test statistics, whose distribution function is obtained either with toy Monte Carlo pseudoexperiments, or using asymptotic analytic expressions [17]. The uncertainties of correlated experimental uncertainties (JES, luminosity,...), across different Higgs channels, are taken into account. A careful treatment of theory uncertainties is also made, again paying attention to those that are correlated, as for example the uncertainty on the Higgs boson production cross-section [15]. Figure 7a summarizes the individual stand-alone exclusion limits associated with the Higgs boson channels discussed in this paper. The result of the combination of these results is shown in figure 7b. The production of a Standard Model Higgs boson is excluded at 95% CL in the mass regions $144 < m_{\mathrm{H}} < 232$ GeV, $256 < m_{\mathrm{H}} < 282$ GeV and $296 < m_{\mathrm{H}} < 466$ GeV. Moreover, the mass regions between 160 and 220 GeV, and between 300 and 420 GeV, are excluded at least with 99% CL.

The exclusion limit in the mass region $110 < m_{\mathrm{H}} < 135$ GeV is given mainly from the combination of the $H \to \gamma\gamma$ and $H \to WW^{(*)} \to l\nu l\nu$ decay channels. For m_{H} up to 180 GeV, the limit is dominated by the $H \to WW^{(*)} \to l\nu l\nu$ decay, while the channels $H \to ZZ \to 4l$ and $H \to ZZ \to ll\nu\nu$ dominate the exclusion limit for $m_{\mathrm{H}} > 180$ GeV.

The expected exclusion covers Standard Model Higgs boson mass range from 131 GeV to 450 GeV. The observed limit is in very good agreement with the background only expected limit over most of the studied mass range, except in the low mass region $130 < m_{\mathrm{H}} < 170$ GeV where the observed limit is consistent with 2σ with the one expected in the hypothesis of no signal. This is mainly due to the results coming from the search for $H \to WW^{(*)} \to l\nu l\nu$ production. More details on this combination are available in this ATLAS public note [21].

The full dataset collected during the 2011 run, more than 5 fb^{-1} for ATLAS and CMS, will definitively help to understand the data better, improve the physics analyses and to increase further the sensitivity to the Higgs boson search to a wider mass interval.

References

[1] Abdelhak Djouadi, *These proceedings*
[2] LEP Working Group for Higgs boson searches, *Phys. Lett.* **B565**, 61 (2003)
[3] Marco Verzocchi, *These proceedings*
[4] ATLAS Collaboration: *J. Instrum.* **3**, 823 (2008)
[5] Vivek Sharma, *These proceedings*
[6] ATLAS Collaboration, *Phys. Lett.* **B705**, 452 (2011), arXiv:1108.5895
[7] ATLAS Collaboration: ATLAS-CONF-2011-103, http://cdsweb.cern.ch/record/1369826
[8] ATLAS Collaboration: ATLAS-CONF-2011-133, http://cdsweb.cern.ch/record/1383836
[9] ATLAS Collaboration: ATLAS-CONF-2011-132, http://cdsweb.cern.ch/record/1383835
[10] ATLAS Collaboration: ATLAS-CONF-2011-134, http://cdsweb.cern.ch/record/1383837
[11] ATLAS Collaboration, *Phys. Lett.* **B705**, 435 (2011), arXiv:1109.5945s
[12] ATLAS Collaboration, *Phys. Rev. Lett.* **107**, 221802 (2011), arXiv:1109.3357
[13] ATLAS Collaboration, *Phys. Lett.* **B707**, 27 (2012), arXiv:1108.5064

[14] ATLAS Collaboration, *Phys. Rev. Lett.* **107**, 231801 (2011), arXiv:1109.3615
[15] LHC Higgs Cross Section Working Group: S Dittmaier *et al*, arXiv:1101.0593 (2011)
[16] A L Read, *N.J. Phys.* **G28**, 2963 (2011)
[17] E Gross, G Cowan, K Cranmmer and O Vitells, *Eur. Phys. J.* **C71**, 1554 (2011)
[18] ATLAS Collaboration: ATLAS-CONF-2011-102, http://cdsweb.cern.ch/record/1369219
[19] M Soldate, J J Van der Bij, R K Ellis and I Hinchliffe, *Nucl. Phys.* **B297**, 221 (1988)
[20] A Pranko, A Safanov, A Elagin and P Murat, *Nucl. Instrum. Methods* **A654**, 481 (2011)
[21] ATLAS Collaboration: ATLAS-CONF-2011-135, http://cdsweb.cern.ch/record/1383838
[22] ATLAS and CMS Collaboration: ATL-PHYS-PUB-2011-011, http://cdsweb.cern.ch/record/1375842